

GREEN SYNTHESIS OF ZnO NANOPARTICLES USING *PHOENIX DACTYLIFERA. L* LEAF EXTRACT: EFFECT OF ZINC ACETATE CONCENTRATION ON THE TYPE OF PRODUCT

D. BARANI^{a,b}, B. BENHAOUA^{c,d,*}, S. E. LAOUINI^b, H. BENTEMAM^a,
N. ALLAG^e, D. BERRA^a, A. GUERRAM^{a,b}

^aFaculty of Technology, Univ. Mohamed kheider, Biskra 07000, Algeria

^bDepartment of Process engineering, Faculty of Technology, University of Echahid Hamma Lakhdar, El Oued 39000, Algeria

^cLab. VTRS, Faculty of Science & Technology, Univ. El-Oued, El oued 39000, Algeria

^dUnit of Renewable Energy Development in Arid Zones (UDERZA), Univ. El-Oued, El Oued 39000, Algeria

^eDepartment of mechanics , Faculty of Technology, University of Echahid Hamma Lakhdar, El Oued 39000, Algeria

In this study, green synthesis of ZnO nanoparticles and single crystals were successfully prepared from *Phoenix Dactylifera.L* leaves extract. Effect of 0.01-0.6M zinc acetate concentration on the nanoparticles and single crystals ZnO formation was studied. UV-Vis, FT-IR spectrophotometer, X-ray diffraction (XRD), scanning electron microscopy (SEM), and EDAX techniques are used for this purpose. UV-Vis absorption spectra exhibited a maximum absorbance plate at 350nm related to the zinc oxide. Optical band gaps values of the ZnO products were closely equal to the bulk one. FT-IR spectra display a feeble peak at 593 and 674cm⁻¹, which are accredited to ZnO vibration. XRD showed a good crystalline quality of the ZnO product with very well defined highest peaks intensities along (002), (100), (101) indexing the hexagonal structure (wurtzite). Deduced grain sizes of the synthesized ZnO nanoparticles were in the range of 19.77-26.28nm. SEM showed that the green synthesizing nanoparticles contain sometimes micro single ZnO crystals. As a result, use of *Phoenix Dactylifera. L* leaves extract offers a low cost and kindly environmentally nanoparticles synthesizing process.

(Received May 22, 2019; Accepted July 18, 2019)

Keywords: ZnO nanoparticles, *Phoenix Dactylifera. L*, Zinc acetate, Green synthesis, XRD

1. Introduction

Because of its increasing application, green synthesis of metal oxide nanoparticles is becoming important as an environmentally friendly choice to conventional manufacturing methods. Currently, research and development in nanotechnology are considered a novelty in modern materials science. Due to their structural, optical, catalytic, electronic, and significant magnetic characteristics [1-3], the nanostructure of transition metal oxides and semiconductors have attracted considerable interest for many research areas such as chemistry, physics, materials science and biotechnology.

Zinc oxide (ZnO) is an important semiconductor due to its adjustable, multifunctional morphological, photonic and spintronic properties [4, 5], which is characterized by a direct broad band space of 3.37eV at room temperature and an energy high excitation of 60meV [6]. The intrinsic properties of ZnO make it an excellent candidate as a potential material in short-wave optoelectronic applications [7]. Also, zinc oxide nanoparticles are easy to produce and are non-toxic and biocompatible; such advantages make them ideal candidates for biological applications [8]. ZnO as materials is successfully applied in a wide range of uses as anti-microbial [9, 10],

* Corresponding author: salah_laouini@yahoo.fr

anticancer in the pharmaceutical industry [11]. It is applied as an ointment due to its antiseptic properties [12], in sunscreens, paints and coatings since to its visible light transparence and high offering UV absorption [13], surface acoustic wave treatment and gas detection [14, 15]. It is also used as UV filter in products for sun protection and LED production [16, 17].

A wide variety of physical and chemical processes have been used to synthesize ZnO: homogenous precipitation techniques [18], sol-gel [19], electrolytic deposition [20], organometallic synthesis [21], microbial wave [22], jet pyrolysis [23], thermal evaporation [24], spray method [25], pulsed laser deposition [26], thermal decomposition [27] and sono chemistry [28]. Several of them are not friendly environmental.

The toxicity of the used chemicals for synthesizing nanoparticles leads to byproducts that can have harmful effects on the environment. The bio synthesis of nanoparticles is a promising method that uses plant extracts for synthesizing metal oxide nanoparticles. Indeed biosynthesis has been demonstrated to be an effective ecological technique to synthesize metal oxide nanoparticles [29]. Therefore, the present study was conducted for the first time to examine the effectiveness of *Phoenix Dactylifera. L* leaves extract with zinc acetate salt in greenly synthesizing ZnO nanoparticles (ZnO NPs). The effect of salt concentration in the extract on elaborated ZnO NPs properties was studied.

2. Materials and methods

2.1. Preparation of the leaf extract

Phoenix Dactylifera. L leaves have been collected from the El Oued region. Fresh leaves were firstly washed several times with tap water, and then followed by distilled water to remove impurities and dust. The obtained leaves were dried in the shade at room temperature for 5-7 days, and then crushed to obtain a fine powder. The later was stored in a container away from the air. The extract was prepared by putting 10g of powder's leaves with 100ml of distilled water in a 500ml glass beaker. The mixture was stirred for 24 hours at room temperature. The extract was filtered by means of a filter paper (Whatman No: 42) and stored in an airtight bottle at 6°C for consequent use.

2.2. Preparation of zinc oxide nanoparticles

Phoenix Dactylifera. L aqueous extract was reacted with six different concentrations of the dehydrating zinc acetate solution ($\text{Zn}(\text{CH}_3\text{COO})_2 \cdot 2\text{H}_2\text{O}$) in an aqueous bath system with continuous stirring at 80°C for 30 minutes. The volume ratio between the leaf extract and the zinc acetate with different concentration (0.01-0.6M) was taken as 100ml/200ml. For each experiment, the formation of zinc oxide nanoparticles is indicated by a change in the color of the mixture solution from green to the dark brown. A few amounts of the as synthesized zinc oxide nanoparticles solution was preserved for UV-visible measurements. The obtained products were collected by centrifugation at 4000 rpm for 15 minutes, then washed with distilled water and dried at 100°C before its annealing at 450°C for 3 hours. The resulting powders were stored in containers for different characterizations.

2.4. Characterization of ZnO nanoparticles

2.4.1. UV-visible spectroscopy

UV-Vis spectroscopy is a technique widely used to examine the optical properties such as the transparence and the gap of the elaborated product. For this Shimadzu UV-Vis spectrophotometer apparatus Model 1800 operating in the range of 200-900nm was used.

2.4.2. FTIR spectroscopy

A Fourier Transform Infrared Spectrophotometer was employed firstly to identify the presence of chemical functional groups in the leaves extract, secondly to study the Zn-O bonds formation after the precipitate annealing at 450°C. For this purpose, Thermo scientific-Nicolet iS5 Total Attenuated Reflectivity (ATR) apparatus operating in the range of 4000-400 cm^{-1} was used.

2. 4. 3. X-Ray Diffraction (XRD)

The crystalline structure of the nanoparticles was studied using X-ray diffractometer (XRD, Mini Flex 600 Rigaku) with $K\alpha$ radiation of copper ($\lambda = 1.5406 \text{ \AA}$) in 2θ range of $20-90^\circ$, whereas X-ray was generated with 30 kilovolts and at 20mA. The structural tasks were done regarding the ZnO Joint Comity Powder Diffraction System (JCPDS) card N° 01.089-0510.

4. Results and discussion

UV-Vis spectra of the as synthesized zinc oxide NPs solution, using *Phoenix Dactylifera*. L leaves extract, are shown in Fig. 1. As can be seen from this figure, plate peak absorption is exhibited at about 350nm, which is attributed to the formation of zinc oxide [3]. An increase in the intensity of the plate peak with the zinc acetate concentration is observed. This may be due to the increasing number of formed nanoparticles because of zinc ions transformations, which may be caused by the complete enlacement of them (zinc ions) by the extract.

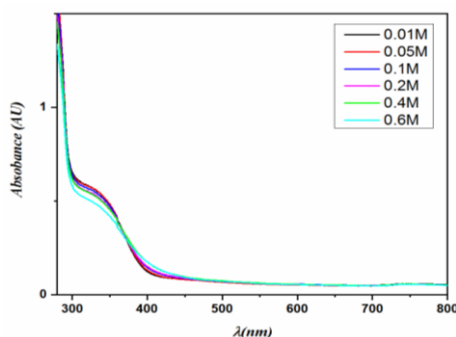


Fig. 1. UV-vis absorbance of the as synthesized zinc oxide nanoparticles solution with different zinc acetate concentration.

What shown in Fig. 2 are the UV-Vis transmittance spectra of the same samples, which for all those were more than 88% in the region (400-900nm). An abrupt decrease in this transmittance in the region below 400nm was observed, which represents the fundamental absorption bands (valence band to conduction band of ZnO nanoparticles). It is worth noting that the estimated optical band gap (E_g) of zinc oxide nanoparticles is generally carried out from this decrease in transmittance using Tauc's relation [30].

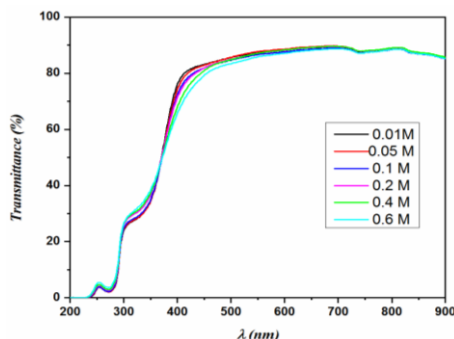


Fig. 2. UV-vis transmittance spectra of the as prepared zinc oxide nanoparticles solution with different concentrations.

Fig. 3 shows the estimated optical band gap (E_g) of the nanoparticles with the help of this relation:

$$(\alpha h\nu)^2 = A(h\nu - E_g) \quad (1)$$

where $h\nu$ is the photon energy, (E_g) is the optical band gap, A is independent constant on $h\nu$. E_g values were deduced from the extrapolating $(\alpha h\nu)^2 = 0$ and illustrated in Table 1, they were found to be ranged in 3.20-3.27eV.

Table 1. Parameters values: d_{hkl} , average grain size, lattice parameters of ZnO green synthesized with different concentration.

Concentration (M)	hkl	2θ (°)	LatticeParameters(Å) $\Delta a = a - a_0, \Delta c = c - c_0$	d (Å) standard	d (Å) calculated	D average (nm)
0.01	100	31.817	$a = 3.2472$	2.81354	2.81258	23.3632
	002	34.418	$c = 5.2151$	2.60270	2.60755	
	101	36.288	$\Delta a = -0.0016$	2.47513	2.47607	
	102	47.518	$\Delta c = 0.0097$	1.91058	1.91348	
0.05	100	31.724	$a = 3.2569$	2.81354	2.82057	19.7798
	002	34.397	$c = 5.2146$	2.60270	2.60732	
	101	36.198	$\Delta a = 0.0081$	2.47513	2.48160	
	102	47.503	$\Delta c = 0.0092$	1.91058	1.91407	
0.1	100	31.724	$a = 3.2281$	2.81354	2.80054	26.2841
	002	34.397	$c = 5.1964$	2.60270	2.59071	
	101	36.198	$\Delta a = 0.0207$	2.47513	2.47059	
	102	47.503	$\Delta c = 0.009$	1.91058	1.91047	
0.2	100	31.724	$a = 3.2281$	2.81354	2.79568	24.4817
	002	34.397	$c = 5.1964$	2.60270	2.59824	
	101	36.198	$\Delta a = 0.0207$	2.47513	2.46410	
	102	47.503	$\Delta c = 0.009$	1.91058	1.90512	
0.4	100	31.957	$a = 3.2301$	2.81354	2.79741	25.4999
	002	34.624	$c = 5.1753$	2.60270	2.58767	
	101	36.365	$\Delta a = 0.0187$	2.47513	2.46225	
	102	47.598	$\Delta c = 0.0300$	1.91058	1.90100	
0.6	100	31.724	$a = 3.2524$	2.81354	2.81674	25.9489
	002	34.397	$c = 5.2032$	2.60270	2.60162	
	101	36.198	$\Delta a = -0.0036$	2.47513	2.47589	
	102	47.503	$\Delta c = 0.0021$	1.91058	1.91060	

Moreover, Urbach energy (E_u), which is directly associated with the disorder in the nanoparticles network, was estimated via F. Urbach relation [31].

$$\alpha = \alpha_0 \exp(h\nu / E_u) \quad (2)$$

where α , $h\nu$, and E_u are the absorption coefficient, the photon energy, and Urbach energy respectively; whereas α_0 is constant. As shown in the inset of Fig. 3, the drawn of $\ln\alpha$ upon the photon energy ($h\nu$) was used to deduce Urbach energy. E_u values were reported in Table 2 they were obtained by inverting the slope of $\ln\alpha$ versus ($h\nu$); values of which are extremely constant (0.1eV) revealing the disorders absence from the network and leads to unvarying band gap.

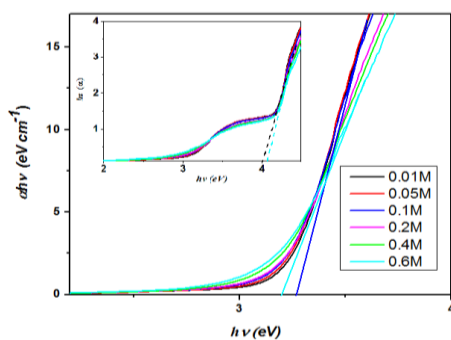


Fig. 3. Band gap (E_g) estimation of the prepared ZnO nanoparticles from Tauc's relation.

Table 2. Optical parameters values: optical gap E_g , Urbach energy E_u , and transmittance of ZnO green s synthesized with different concentration.

Concentrations(M)	Optical gap E_g (eV)	Urbach energy E_u (meV)	Transmittance (%)
0.01	3,21	100	90
0.05	3,22	108	88.88
0.1	3,27	104	88.74
0.2	3,23	117	88.50
0.4	3,25	121	88.38
0.6	3,20	135	88.14

FT-IR study was used to find the possible biomolecules in *Phoenix dactylifera*. L extract involved in the formation and stabilization of ZnO NPs. The possible functional groups of the extract before it use are shown in Fig. 4. Also in this figure, the absorption spectra of the prepared ZnO NPs and the extract after it use in preparing ZnO NPs (case of 0.4M of Zn $(\text{CH}_3\text{COO})_2 \cdot 2\text{H}_2\text{O}$ sample) were exhibited. For the synthesized and annealed ZnO NPs samples at 450°C , adsorption peaks at 593 and 674 cm^{-1} are allotted to green synthesized ZnO NPs [32]. Furthermore, the FT-IR spectrum of the extract before it use show strong peaks and bands at 3422 , 2934 , 1631 , 1402 , 1208 , and 1070 cm^{-1} . The most remarkable wide stretching vibration band correspond to 3422 cm^{-1} is related to free O—H in molecule and O—H group bonds. The bands at 2934 , 1631 , 1402 and range from 1208 to 1070 cm^{-1} represent the C—H saturated hydrocarbons ($\text{C}_{\text{sp}^3}\text{-H}$), carbonyl group (C=O), stretching C=C aromatic ring, and C—OH bonds, respectively. While the band around 2354 cm^{-1} corresponds to CO_2 vibration mode [33], which may be getting into the extract, from its surrounding environment. FT-IR spectrum of the extract after it use shows remarkable diminish in 3422 cm^{-1} wide stretching vibration band which is related to disappearances of O—H bonds from the used extract. A similar diminish in the bands at 2934 , 1631 , 1402 and 1208 to 1070 cm^{-1} representing the above cited bonds was remarked. As it is well known phenolic compounds contain bonds such as C=C, C—H, and C—OH with of course radicals and based on previous study [34] in which it was shown that disappearance of cited bands between 3422 and 1070 cm^{-1} , are credited to the phenolic compounds, which were involved in the formation of copper oxides NPs. Such conceptions lead us to proclaim that the agents responsible for the formation of ZnO NPs and single crystal are the phenolic compounds. It is worth noting that an appearance of peaks at 593 and 674 cm^{-1} in the extract spectrum after its use may be assigned to residual ZnO NPs in the extract.

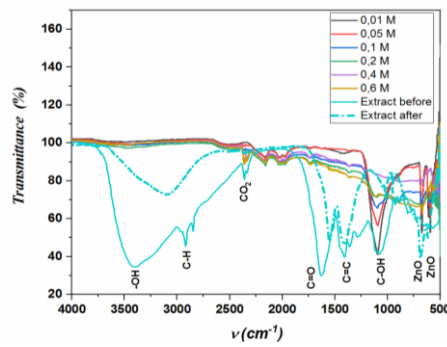


Fig. 4. FTIR spectrum of *Phoenix dactylifera*. L extract and the prepared ZnO nanoparticles as function of concentration.

Fig. 5 exhibits XRD patterns of the synthesized and annealed at 450°C ZnO nanoparticles with different concentrations of zinc acetate. It is clearly seen that diffraction peaks are present in all sample spectrum. Various crystal planes such as (100), (002), (101), (102), (110), (103), (200), (112), (201), (202), (104) and (203) are matching well with the ZnO hexagonal wurtzite structure having JCPDS Card No. 01.089-0510. (100), (002), and (101) peaks intensities increase slightly with increasing zinc acetate concentration in the solution till 0.4M then decrease for the last concentration. The presence of peaks (100), (002) and (101) in the XRD spectrum indicates the formation of the high purity of crystallinity of the ZnO nanoparticles [35]. Moreover, no peak was observed due to other impurities.

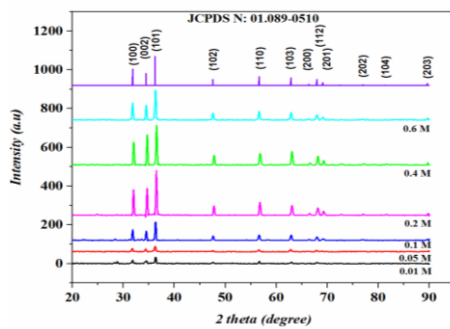


Fig. 5. X-ray diffraction patterns of ZnO nanoparticles as function of concentration.

The average crystallite size was estimated according to the Scherrer equation [36].

$$D = \frac{0.9\lambda}{\beta \cos \theta} \quad (3)$$

where D is the crystallite size, β the full width at half-maximum width (FWHM) of the most intense diffraction peak, λ the X-ray wavelength (1.5406 Å) and θ is the Bragg angle, as reported in Table 1 and plotted in Fig. 6, the average crystallite size was found to be in the range of 19.77-26.28 nm.

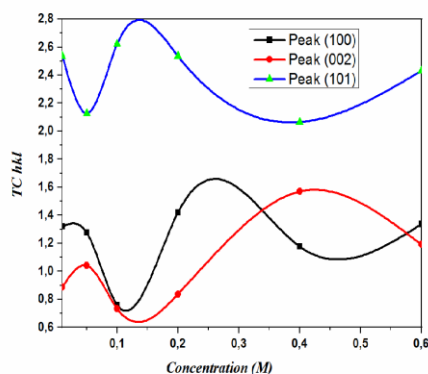


Fig. 6. Grain size with different concentration of zinc acetate.

Different texture coefficients $TC(hkl)$ that measure the relative degree of preferred orientation among the crystal planes, were calculated from X-ray data using the following formula [37, 38]:

$$TC(hkl) = \frac{I(hkl)/I_0(hkl)}{N^{-1} \sum_n I(hkl)/I_0(hkl)} \quad (4)$$

where $I(hkl)$ is the measured relative intensity of (hkl) plane in this work, $I_0(hkl)$ is the standard intensity of the considered (hkl) plane taken from JCPDS data, N is the reflection number and n is the number of diffraction peaks (in this work is equal to 9). For different concentrations, only $TC(hkl)$ values of (002) , (100) , (101) , which are the highest peaks intensities are shown in Fig. 7.

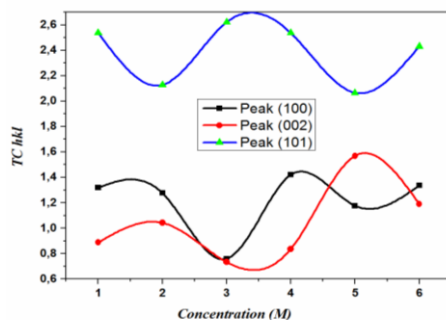


Fig. 7. Texture coefficient of ZnO nanoparticles with different concentration.

The lattice parameters (a and c) are given as follow [39]:

$$2d_{hkl} \sin(\theta) = n\lambda \quad (5)$$

and

$$\frac{1}{d_{hkl}^2} = \frac{4}{3a^2} (h^2 + k^2 + hk) + \frac{l^2}{c^2} \quad (6)$$

where d_{hkl} and (hkl) are the interplanar distance and the Miller indices, respectively. The lattice constants (a and c) are shown in Table 1. They are closely equal to those of the JCPDS card N°

01.089-0510, ($a_0 = b_0 = 3.2488 \text{ \AA}$ and $c_0 = 5.2054 \text{ \AA}$) are for instance in the case of 0.1M sample ($a = b = 3.2472 \text{ \AA}$, $c = 5.1964 \text{ \AA}$).

Fig. 8 (a-f) exhibits SEM images of the synthesized ZnO NPs. It is clearly showed that, in general, the nanoparticles are more depending with the zinc acetate concentration. Different irregular shapes are observed; a mixture of dried cotton like and sheets (Fig. 8 a and b) in the cases of the concentrations (0.01 and 0.05M). Whereas for 0.2 and 0.6 M, the nanoparticles become greater and have fleece wool shapes as seen in (Fig. 8 d and f). But, for the 0.1 and 0.4M concentration of zinc acetate, as depicted in their SEM images (Fig. 8 c, c', e and e' (magnified)), it was observed that there is more than one shape (long stick forms nanoparticles and having only longitudinal shape) and even they become greater in dimension and containing, sometimes, single microcrystals (Fig. 8 c' and e').

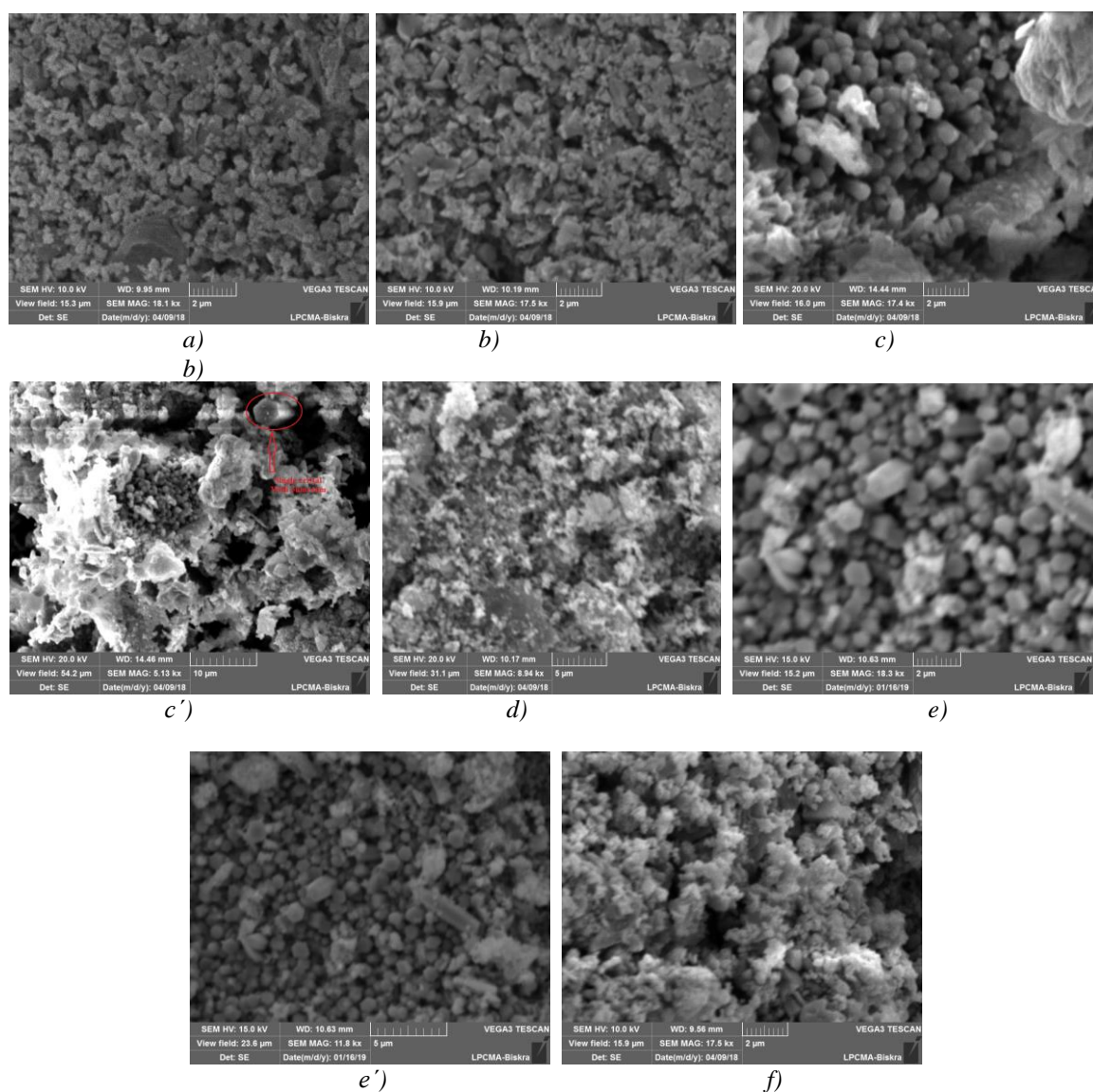


Fig. 8. SEM and EDAX images of green synthesized ZnO nanoparticles: a) 0.01 M, b) 0.05 M, c) 0.1 M, c') 0.1 M focused image, d) 0.2 M, e) 0.4 M, e') 0.4 M focused image, f) 0.6 M

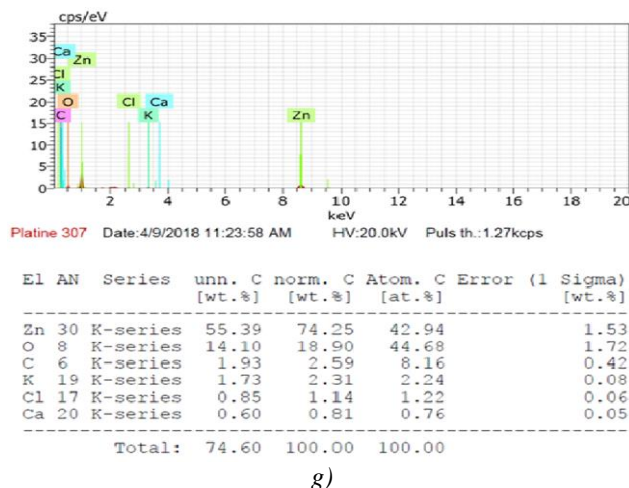


Fig. 8. SEM and EDAX images of green synthesized ZnO nanoparticles:
g)EDAX of ZnO nanoparticles.

Further analysis of Zinc oxide nanoparticles, by EDAX as shown in Fig. 8 g and its associated data, confirms the presence of zinc and oxygen, with the weight percentage of about 42.94% Zn and 44.68% O.

As a result to this green synthesized zinc oxide NPs, it seems to us that the amount of zing acetate (ratio of acetate/leaf extract) plays a key role in producing and stabilizing the zinc oxide NPs. It has found that by increasing the ratio, the shape and size of nanoparticles change too; sometimes leads to ZnO single crystal formation. Only as information, the green reduction of the zinc salts starts rapidly, and the formation of zinc oxide nanoparticles is indicated by changes in the mixture solution color from green to the dark brown as it was observed in previous work of green synthesized copper oxide NPs [34]. Based on the presence of the absorbance bands at 3264, 1605, 1442, 1283 and 1049 cm^{-1} of polyphenols then its disappearance from the extract after its use as seen in Fig.4, it seems to us that the latter has the foremost role in stabilizing the zinc oxide NPs and the micro single crystal.

4. Conclusion

In this study, ZnO nanoparticles and single crystal were successfully prepared from *Phoenix Dactylifera*.L leaves extract for the first time. Effect of zinc acetate concentration in the range of (0.01-0.6 M) on the nanoparticles formation was studied. The optical band gap, E_g , values were found to be ranged in 3.20-3.27eV closely to the bulk one. XRD shows the good crystalline quality of the ZnO product with very well defined peaks along (002), (100), (101), which are the highest peaks intensities and indexed as a hexagonal structure (wurtzite). The grain sizes of the synthesized ZnO nanoparticles are in the range of 19.77-26.28 nm. SEM showed that the green synthesizing nanoparticles contain sometimes ZnO single crystals having as dimension more than $4\mu\text{m} \times 3\mu\text{m}$ which was obtained with zinc acetate concentration of 0.1 and 0.4M. Use of *Phoenix Dactylifera*. L leaves extract offers a low cost and friendly environmentally nanoparticles synthesis way. The variation of the zinc acetate concentration allows us to strictly control the size and shape of the ZnO nanoparticles.

Acknowledgments

This work was supported in part by UDERZA Unit of El-Oued University; we thank Madame Karoui RADJA for his help and assistance to measure UV-Visible data. X-ray diffraction

data in this work were acquired with an instrument supported by the University of Biskra. We thank B. Gasmi (Biskra University) for the assistance in XRD data acquisition. We thank also Youcef MEFTAH (Lab: VTRS El-Oued University) for her assistance in the organization of the manuscript and the helpful discussion.

References

- [1] G. Singhal, R. Bhavesh, K. Kasariya, A. R. Sharma, R. P. Singh, *Journal of Nanoparticle Research* **13**(7), 2981 (2011).
- [2] C. Vidya, S. Hiremath, M. Chandraprabha, M. L. Antonyraj, I. V. Gopal, A. Jain, K. Bansal, *Int. J. Curr. Eng. Technol.* **1**, 118 (2013).
- [3] S. Talam, S. R. Karumuri, N. Gunnam, *ISRN Nanotechnology* **2012** (2012).
- [4] F. Thema, E. Manikandan, M. Dhlamini, M. Maaza, *Materials Letters* **161**, 124 (2015).
- [5] F. Kaminsky, *Earth-Science Reviews* **110**(1-4), 127 (2012).
- [6] S. J. Yang, C. R. Park, *Nanotechnology* **19**(3), 035609 (2007).
- [7] A. Diallo, B. Ngom, E. Park, M. Maaza, *Journal of Alloys and Compounds* **646**, 425 (2015).
- [8] P. Jamdagni, P. Khatri, J. Rana, *Journal of King Saud University-Science* **30**(2), 168 (2018).
- [9] A. B. P. Jiménez, C. A. H. Aguilar, J. M. V. Ramos, P. Thangarasu, *Australian Journal of Chemistry* **68**(2), 288 (2015).
- [10] A. Shah, E. Manikandan, M. B. Ahamed, D. A. Mir, S. A. Mir, *Journal of Luminescence* **145**, 944 (2014).
- [11] L. He, Y. Liu, A. Mustapha, M. Lin, *Microbiological research* **166**(3), 207 (2011) .
- [12] C. Joel, M. S. M. Badhusha, *Der Pharmacia Lettre* **8**(11), 218 (2016) .
- [13] N. M. Franklin, N. J. Rogers, S. C. Apte, G. E. Batley, G. E. Gadd, P. S. Casey, *Environmental science & technology* **41**(24), 8484 (2007) .
- [14] S. Kalusniak, S. Sadofev, J. Puls, F. Henneberger, *Laser & Photonics Reviews* **3**(3), 233 (2009).
- [15] Y. Li, J.Z. Zhang, *Laser & Photonics Reviews* **4**(4), 517 (2010) .
- [16] U. Ozgur, D. Hofstetter, H. Morkoc, *Proceedings of the IEEE* **98**(7), 1255 (2010) .
- [17] K. Schilling, B. Bradford, D. Castelli, E. Dufour, J. F. Nash, W. Pape, S. Schulte, I. Tooley, J. Van Den Bosch, F. Schellauf, *Photochemical & Photobiological Sciences* **9**(4), 495 (2010).
- [18] J. H. Kim, W. C. Choi, H. Y. Kim, Y. Kang, Y.-K. Park, *Powder technology* **153**(3), 166 (2005).
- [19] H. Çolak, E. Karaköse, *Journal of Alloys and Compounds* **690**, 658 (2017) .
- [20] M.-H. Wang, X.-Y. Ma, F. Zhou, *Materials Letters* **142**, 64 (2015) .
- [21] J. Y. Park, Y. S. Yun, Y. S. Hong, H. Oh, J.-J. Kim, S. S. Kim, *Synthesis, Applied Physics Letters* **87**(12), 123108 (2005).
- [22] S. D. Abraham, S. T. David, R. B. Bennie, C. Joel, D. S. Kumar, *Journal of Molecular Structure* **1113**, 174 (2016) .
- [23] R. K. Sonker, S. Sabhajeet, S. Singh, B. Yadav, *Materials Letters* **152**, 189 (2015).
- [24] T. Tani, L. Mädler, S. E. Pratsinis, *Journal of Nanoparticle Research* **4**(4), 337 (2002).
- [25] M.-T. Chen, J.-M. Ting, *Thin Solid Films* **494**(1-2), 250 (2006).
- [26] Y. Wang, W. Ding, H. Wang, S. Peng, Y. Wang, W. Chai, *Materials Letters* **149**, 37 (2015).
- [27] B. Yao, Y. Chan, N. Wang, *Applied Physics Letters* **81**(4), 757 (2002).
- [28] G. K. Mani, J. B. B. Rayappan, *Materials Letters* **158**, 373 (2015) .
- [29] N. Thovhogi, A. Diallo, A. Gurib-Fakim, M. Maaza, *Journal of Alloys and Compounds* **647**, 392 (2015).
- [30] F. Urbach, *Physical Review* **92**(5), 1324 (1953).
- [31] J. Tauc, R. Grigorovici, A. Vancu, *Physica Status Solidi B* **15**(2), 627 (1966) .
- [32] A. C. Taş, P. J. Majewski, F. Aldinger, *Journal of the American Ceramic Society* **83**(12), 2954 (2000).
- [33] V. Bharathi, M. Sivakumar, R. Udayabhaskar, H. Takebe, B. Karthikeyan, *Applied Physics A* **116**(1), 395 (2014).
- [34] D. Berra, S. Laouini, B. Benhaoua, M. Ouahrani, D. Berrani, A. Rahal, *Digest Journal of*

- Nanomaterials and Biostructures **13**(4), 1231(2018).
- [35] P. Nethravathi, G. Shruthi, D. Suresh, H. Nagabhushana, S. Sharma, *Ceramics International* **41**(7), 8680 (2015).
- [36] P. Scherrer, Bestimmung der inneren Struktur und der Größe von Kolloidteilchen mittels Röntgenstrahlen, *Kolloidchemie Ein Lehrbuch*, Springer1912, pp. 387-409.
- [37] G. Leonhardt, V. V. Nemoshkalenko, V. G. Aleshin. *Electron Spectroscopy of Crystals* **16**(9), 982 (1981).
- [38] P. Paufler, C. S. Barrett, T. B. Massalski, *Kristall und Technik* **16**(9), 982 (1981).
- [39] L. Dghoughi, B. Elidrissi, C. Bernede, M. Addou, M. A. Lamrani, M. Regragui, H. Erguig, *Applied Surface Science* **253**(4), 1823 (2006).